

Dipolariton propagation in a van der Waals TMDC with Ψ -shaped channel guides and buffered channel branches

Patrick Serafin¹ and German V. Kolmakov¹

¹*Physics Department, New York City College of Technology,
The City University of New York, Brooklyn, New York 11201, USA*

(Dated: June 24, 2022)

Using a computational approach based on the driven diffusion equation for dipolariton wave packets, we simulate the diffusive dynamics of dipolaritons in an optical microcavity embedded with a transition-metal dichalcogenide (TMDC) heterogenous bilayer encompassing a Ψ -shaped channel. By considering exciton-dipolaritons, which are a three way superposition of direct excitons, indirect excitons and cavity photons, we are able to drive the dipolaritons in our system by the use of an electric voltage and investigate their diffusive properties. More precisely, we study the propagation of dipolaritons present in a MoSe_2 - WS_2 heterostructure, where the dipolariton propagation is guided by a Ψ -shaped channel. We also consider the propagation of dipolaritons in the presence of a buffer in the Ψ -shaped channel and study resulting changes in efficiency. By our consideration of a geometrically novel dipolariton channel guide, we introduce novel designs for optical routers at room temperature as well as replicate the dipolariton redistribution efficiencies of previously proposed polaritronic applications.

I. INTRODUCTION

Recent advances in the field of polaritronics have enabled us to realize many proposed application of exciton and polariton physics at room temperature scales¹. Exciton-polariton physics has already found its application in devices such as lasers², optical transistors^{3,4} and light emitting diodes⁵. The wide array of phenomena found in exciton-polariton physics, such as superfluidity⁶⁻⁸ and Bose-Einstein condensate^{9,10} has drawn attention towards research into their implementation in various systems as well as potential applications¹¹.

Some obstacles that can arise with the use of conventional polaritons, such as low exciton binding energies and electrical neutrality can be remedied by the use of charged quasi-particles; that is, dipolaritons in van der Waals transition metal dichalcogenide (TMDC) heterostructures. Dipolaritons present us with the possibility of being driven by an external voltage, something that is not possible in a conventional polariton as it is electrically neutral. The emergence of Van der Waal TMDC heterostructures enables us to use properties such as large binding energies and large Rabi splitting energies¹² to transfer proposed applications of polaritons to room temperature scales. In addition, these TMDC heterostructures provide for a type-II band alignment¹³ which enables one to spatially separate electrons and their respective holes upon laser pumping into the system.

In this paper, the diffusive dynamics of dipolaritons present in a TMDC inside of an optical microcavity is computationally modeled. In particular, we consider heterostructures with a Ψ -shaped channel guide in contrast to heterostructures with Y-shaped channel guides previously investigated for identical system parameters³. This MoSe_2 - WS_2 heterogenous bilayer embedded inside of a optical microcavity enables one to redistribute dipolaritons through the Ψ -shaped channel guide using an exter-

nal voltage as shown in Fig.1. The system parameters for this redistribution are investigated in order to determine the conditions that optimize the efficiency of redistribution of the dipolariton gas in our system. By considering a novel Ψ -shaped channel guide, we are able to compare efficiency between geometrically different channel guides. In particular, by considering various driving forces, electric field angles, and channel buffers we can establish optimal system parameters that promote efficient dipolariton routing in the Ψ -shaped channel of the TMDC.

II. SIMULATION METHOD

We model our system of dipolariton propagation in a TMDC with a Ψ -shaped channel using previously considered models for dipolariton based optical transistors using TMDC's³. In particular, we consider the propagation of dipolaritons controlled by an external electric field E generated by an external voltage acting on the charges found in the MoSe_2 layer of the TMDC heterostructure as seen in Fig.1. In our approach, we consider the diffusive dynamics of the dipolariton gas at scales much larger than the dipolariton mean path and describe the dipolariton gas using the quasi-classical stochastic driven dissipative diffusion equation for a polariton wave packet.¹⁴:

$$d\mathbf{r} = \eta_{\text{dip}} \mathbf{F}(\mathbf{r}(t), t) dt + \sqrt{2D} d\xi(t) \quad (1)$$

The first term in Eq.(1) $\mathbf{F}(\mathbf{r}, t)$ represents the external force acting on the dipolaritons, the second term η_{dip} is the dipolariton mobility, whilst D is the diffusivity, and $d\xi(t)$ the differential of a Weiner process¹⁴. The force acting on polaritons is set to $\mathbf{F} = -\nabla U_{\text{eff}}(r)$. Polariton addition to the system is modeled using δt which represents a Gaussian probability distribution. Eq.(1) has

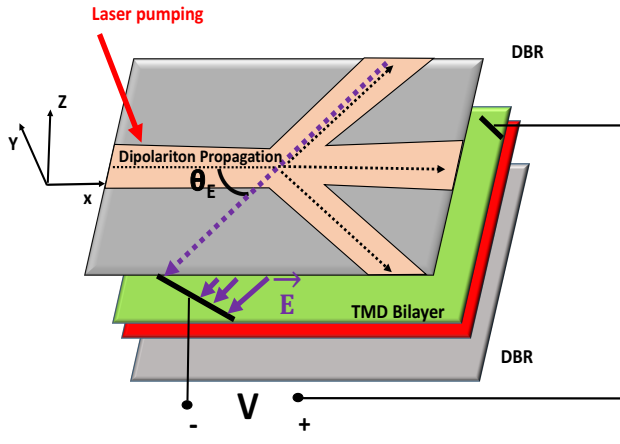


FIG. 1. Schematic of a TMD heterogenous bilayer embedded inside an optical microcavity with a Ψ -shaped channel guiding the dipolaritons. The opening angle of the channel relative to the middle branch is $\theta_0 = 30$ and the direction of the field \mathbf{E} generated by an external voltage applied to the bilayer is defined by an angle θ_E between the field vector and the direction of the stem of the Ψ -shaped channel. The direction of the electric driving force applied to the dipolaritons is opposite to the direction of the electric field. Distributed Bragg Reflectors (DBR) are placed between the TMD bilayer and laser pumping is applied to generate dipolaritons, at the beginning of the stem of the channel at which point they propagate along the x -axis towards the junction under the action of the electric field \mathbf{E} .

been shown to provide many advantages, among them being computational effectiveness for a system of large particles and off lattice properties¹⁵. The stochastic nature of Eq.(1) has been applied in other models such as ones studying the diffusive properties of gases¹⁶ and nanoparticles in fluids¹⁷. This computational model follows the same physics and identical system parameters as described when considering this system with a Y-shaped channel guide³. The model parameters are summarized in table 1 and their properties and derivations can be found in investigations of similar systems^{3,14}.

To characterize the propagation of the dipolaritons in the channel, we numerically counted the total number of particles n , present in each branch of the Ψ -shaped channel at locations $x_n \geq 450\mu\text{m}$, where x_n is chosen in such a manner as to only count particles that have propagated at a sufficient distance through the junction of the channel.

To characterize the redistribution of the dipolaritons in each branch of the channel, we calculated the fraction of dipolaritons propagating through the upper branch of the channel, or what we define as the efficiency in the

TABLE I. Simulation parameters for a cavity with embedded MoSe₂-WS₂ bilayer

Quantity name	Value	Variable
Exciton mass	m_{ex}	$0.70m_0$
Photon mass	m_{ph}	$1.1234 \times 10^{-5}m_0$
Dipolariton mass	m	$2.4 \times 10^{-5}m_0$
Dipolariton lifetime	τ_{dip}	$15.64 \times 10^{-12} \text{ s}$
Indirect exciton lifetime	τ_{IX}	$80 \times 10^{-12} \text{ s}$
Direct exciton lifetime	τ_{DX}	$4.0 \times 10^{-12} \text{ s}$
Cavity Photon lifetime	τ_{ph}	$100 \times 10^{-12} \text{ s}$
Exciton diffusion coefficient	D_{ex}	$14 \text{ cm}^2/\text{s}$
Dimensionless dipolariton diffusion coefficient	$D \times dt/dx^2$	271.7
Dimensionless dipolariton mobility	$\eta_{\text{dip}} \times eVdt/dx$	0.0015
Dielectric constant	ϵ	4
Exciton Energy	E_{ex}	1.58eV
Confining potential	U	$25 - 500\text{meV}$
Numerical unit of length	dx	$0.15 \mu\text{m}$
Numerical time step	dt	9.63 fs

channel,

$$\varepsilon = \frac{n_{\text{up}}}{n_{\text{up}} + n_{\text{mid}} + n_{\text{low}}} \times 100\%. \quad (2)$$

where n_{up} is the number of dipolaritons in the upper branch of the channel, n_{mid} is the number of dipolaritons in the middle branch of the channel, n_{low} is the number of dipolaritons in the lower branch of the channel. Fig.2 provides for an illustration of the density of dipolariton particles in the Ψ -shaped channel for the specified cases.

We define ε in such a manner in order to find the percentage of dipolaritons distributed through the upper branch of the channel relative to the total number of dipolaritons in the Ψ -shaped channel. This enables us to quantify to what extent we can re-route the total number dipolaritons in the channel through the upper branch of the Ψ -shaped channel. Thus, we can claim that a higher value for ε will indicate a greater ability to drive the dipolaritons through the desired branch of the Ψ -shaped channel.

Furthermore, we also investigate the efficiency of the channel when the middle branch of the Ψ -shaped channel is taken to be a buffer, such that the density of dipolaritons through the middle branch is not considered in the calculation in what we define as the buffered efficiency, ε_2 . This consideration gives us an efficiency compari-

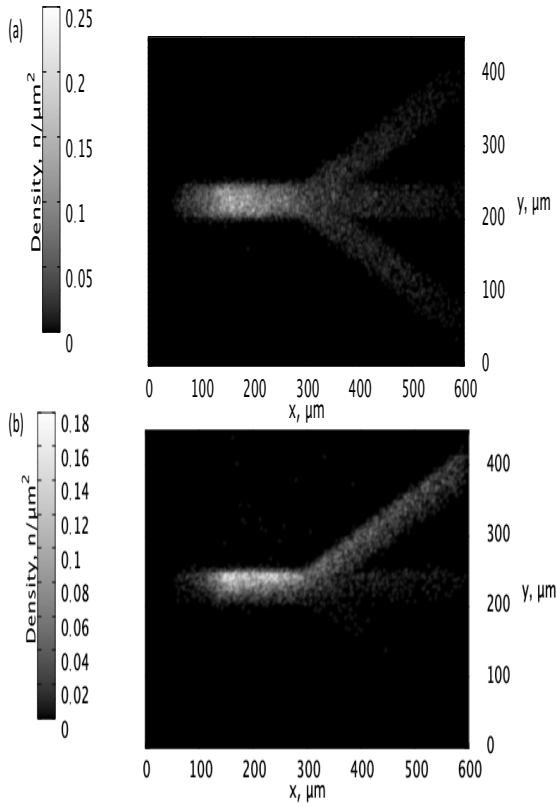


FIG. 2. Dipolariton propagation through the three branches of the Ψ channel for the case of (a) $F=0.5\text{eV/mm}$ and $\theta_E = 0$ (b) $F=2.0\text{eV/mm}$ and $\theta_E = 60^\circ$

son of a Ψ -shaped channel to that of Y-shaped channel for the case when the angle between the upper and lower branches is sixty, where for certain cases dipolaritons were able to be re-routed through the upper branch of the channel with greater than 90% efficiency³. Thus, the buffered efficiency ε_2 for the channel in this case is calculated as,

$$\varepsilon_2 = \frac{n_{\text{up}}}{n_{\text{up}} + n_{\text{low}}} \times 100\%. \quad (3)$$

III. OPTIMIZING THE EFFICIENCY OF THE Ψ CHANNEL TO EFFECTIVELY REROUTE DIPOLARITONS

In order to determine the optimal conditions for directing dipolaritons in the Ψ -shaped channel, we varied the electric field angle θ_E in our system and calculated the resulting efficiency in the channel. In order to test the efficacy of changing the electric field angle θ_E on ε , we varied the electric field angle from $\theta_E = 0^\circ$ to $\theta_E = 60^\circ$. The result of increasing the electric field angle on efficiency at constant driving force can be shown in Fig.3(a) where we can observe the dipolariton particle number

and the channel efficiency as functions of channel electric field angle for the case of a fixed electric driving force of $F=2.0\text{eV/mm}$. We see in Fig.3(a) that an increase in the electric field leads to a monotonic increase in efficiency. In particular we can see that as the electric field angle θ_E is increased from $\theta_E = 0^\circ$ to $\theta_E = 90^\circ$, the efficiency ε is improved by $\approx 70\%$. Furthermore, we can observe that total number of particles in the upper branch n_{up} increases from 1.5×10^4 particles to 7×10^4 particles as the electric field angle θ_E is increased from $\theta_E = 0^\circ$ to $\theta_E = 90^\circ$. We can also observe that the number of particles present in the lower branch of the channel n_{low} decreases from 3.3×10^3 particles to 1×10^2 particles as θ_E is increased from $\theta_E = 0^\circ$ to $\theta_E = 90^\circ$. In addition Fig.3(a) shows that the number of particles going through the middle branch of the channel increase from 5.3×10^3 particles to 1.2×10^4 particles as the electric field angle is increased from $\theta_E = 0^\circ$ to $\theta_E = 90^\circ$. Thus, increasing the electric field angle in our Ψ -shaped channel from $\theta_E = 0^\circ$ to $\theta_E = 90^\circ$ with the driving force $F = 2.0\text{eV/mm}$ provides for an efficiency of $\approx 85\%$. This improvement of efficiency as the electric field angle is increased can be attributed to the fact that as the angle is placed more level to the direction of the upper channel branch the dipolaritons have a greater statistical probability to be driven through the upper and middle branch of the channel rather than the lower branch of the channel. When the electric field angle is set to zero, there is no driving direction and thus the dipolaritons will propagate stochastically through the channel's branches. Thus, we can claim that increasing the electric field angle in the channel improves efficiency, while increasing the upper branch population and decreasing the lower branch population of dipolaritons.

In order to determine the efficiency of the channel in the presence of a buffer channel, we numerically calculated the buffered efficiency ε_2 as a function of the electric field angle θ_E . In particular, we considered the middle branch of the Ψ -shaped channel to not be considered in our calculation for ε_2 as seen in Eq.(3). In Fig.3(b) we can observe the dipolariton particle number and the channel efficiency as functions of channel electric field angle for the case of a fixed electric driving force of $F=2.0\text{eV/mm}$. In particular we can observe that as the electric field angle θ_E is increased from $\theta_E = 0^\circ$ to $\theta_E = 90^\circ$ the efficiency with buffer ε_2 increases monotonically with an increase with the electric field angle θ_E . In Fig.3(b) we can see that ε_2 is maximized for the case of $\theta_E = 90^\circ$ where we can obtain a buffered efficiency of $\varepsilon_2 \approx 100\%$ and total particle number of 7×10^4 particles. Thus, increasing the electric field angle from $\theta_E = 0^\circ$ to $\theta_E = 90^\circ$ provides for a $\approx 18\%$ improvement of ε_2 with 5.4×10^3 particles in the upper branch n_{up} . Compared to the case of no buffer, we see that increasing the electric field angle with a buffer in the Ψ -shaped channel has a lower impact on the improvement of efficiency while

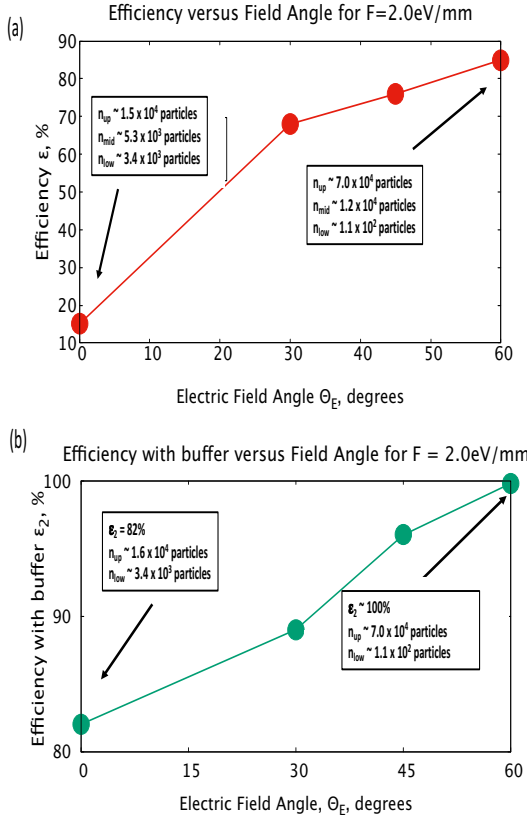


FIG. 3. (a) Channel efficiency ε versus the electric field angle θ_E for the case of fixed driving force $F = 2.0\text{eV/mm}$ and (b) Buffered channel efficiency ε_2 versus θ_E for the case of a fixed driving force $F = 2.0\text{eV/mm}$

clearly leaving particle number unchanged. Thus, we can state that considering a buffer in the middle branch of the Ψ -shaped channel makes the channel similar geometrically that of a Y-shaped channel with a similar redistribution efficiency³

To determine the optimal conditions for directing dipolaritons in the Ψ -shaped channel, we varied the driving force F in our system and studied the resulting distribution of dipolaritons in our system. In Fig.4(a) we can see the efficiency ε as a function of the driving force F for the case of a fixed electric field angle $\theta_E = 60^\circ$. We can observe that the efficiency ε is a monotonically increasing function with the driving force F where ε is maximized at a value of $\approx 85\%$ when the driving force is set to $F = 2000\text{meV/mm}$. In particular we can see that as the driving force F is increased from 500meV/mm to 2000meV/mm , the efficiency ε is improved by $\approx 20\%$. This improvement in efficiency is noted as less substantial than the improvement we can gain by increasing the electric field angle as previously discussed. In addition, we can see in Fig.4(a) that as the driving force F is increased from 500meV/mm to 2000meV/mm , the the number of particles present in the upper branch of the channel increases from 3.1×10^3 particles to 7×10^4 particles,

whilst the number of particles present in the lower branch of the channel decreases from 2×10^2 particles to 1×10^2 particles. This effect can be attributed to the fact that as the electric driving force on the dipolaritons is increased, there are more particles directed towards the direction of the field angle. Thus, we can claim that an increase in the electric field angle in the channel increases the efficiency ε in the channel, while increasing the total upper branch particle population and lowering the lower branch dipolariton population

In order to determine the efficiency of the channel in the presence of a buffer channel, we numerically calculated the buffered efficiency ε_2 as a function of the driving force F . In particular, we considered the middle branch of the Ψ -shaped channel to not be considered in our calculation for ε_2 as seen in Eq.(3). In Fig.4(b) we can see the efficiency ε_2 of the Ψ -shaped channel with a buffer as a function of the driving force, F for the case of $\theta_0 = 60^\circ$. We can observe in Fig.4(b) that the efficiency ε_2 is maximized when the driving force F is set to $F = 2000\text{meV/mm}$ where we find a buffered efficiency of $\approx 99\%$. Thus we can claim an improvement in buffered efficiency of $\approx 5\%$ as the driving force F is increased from 500meV/mm to 2000meV/mm . This improvement in efficiency is noticeably less significant when compared to the improvement we obtain with an increase of driving force for the case with no buffer as the starting efficiency for the case of the buffer is already quite high at $\varepsilon_2 \approx 95\%$. Thus, we can report that an increase of the channel electric driving force improves the buffered efficiency; however, this effect is not a substantial as the effect of increasing driving force in the unbuffered channel.

IV. CONCLUSIONS

The optimum efficiency ε for an unbuffered Ψ -shaped TMDC channel has been shown to be maximized at particular values of θ_E and F . In particular, for values of $F = 2.0\text{eV/mm}$ and $\theta_E = 60^\circ$, we can re-route $\approx 85\%$ of dipolaritons through the upper branch of the unbuffered channel. When considering a buffered channel, we are able to re-route $\approx 100\%$ of dipolaritons as demonstrated in other geometrically similar channels when the channel parameters are set to $F = 2.0\text{eV/mm}$ and $\theta_E = 60^\circ$ ³. For all cases considered, ε and ε_2 were shown to be monotonically increasing functions with an increase of F as well as an increase of θ_E . The impact of increasing driving force and electric field angle was less substantial on ε_2 when compared to ε . These results closely resemble the results when considering Y-shaped channel guides³, with efficiencies over 95% at optimal parameter ranges. Our results demonstrate the possibility of replicating other proposed designs of optical transistors in TMDC materials, whilst also opening the route toward the design of novel optoelectronic applications using Ψ -shaped channel guides and buffered channels.

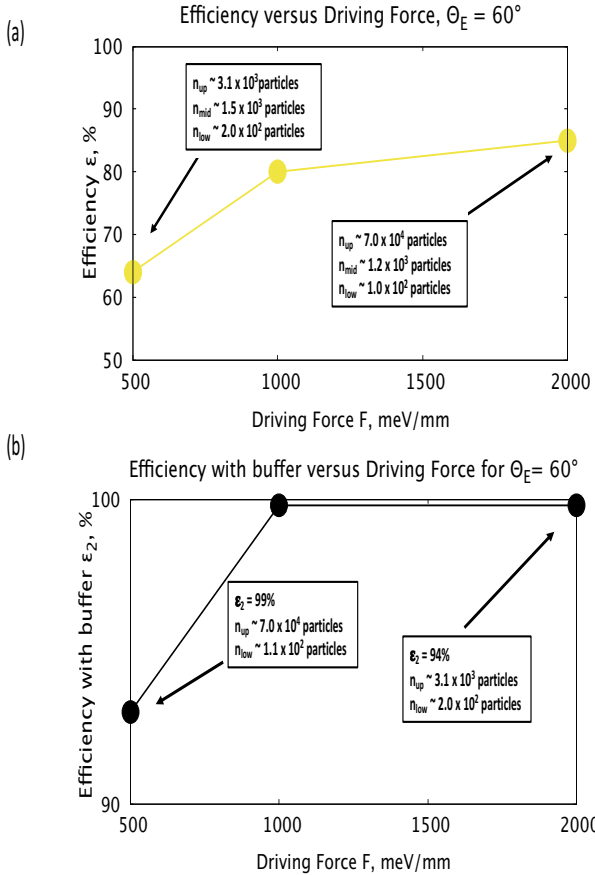


FIG. 4. (a) Channel efficiency ϵ versus the driving force F for the case of a fixed electric field angle $\theta_E = 60^\circ$ and (b) Buffered channel efficiency ϵ_2 versus the driving force F for the case of a fixed electric field angle $\theta_E = 60^\circ$

V. ACKNOWLEDGMENTS

This work was supported in part by the Department of Defense under the grant No. W911NF1810433. The authors are grateful to The Center for Theoretical Physics of New York City College of Technology of The City University of New York for providing computational resources. The authors are also grateful to R. Ya. Kezerashvili, O. L. Berman, T. Byrnes for fruitful discussions.

VI. REFERENCES

- 1 S. I. Tsintzos, N. T. Pelekanos, G. Konstantinidis, Z. Hatzopoulos, and P. G. Savvidis. A GaAs polariton light-emitting diode operating near room temperature. *Nature*, 453(7193):372–375, 2008.
- 2 S. Christopoulos, G. Baldassarri Höger von Högersthal, A. J. D. Grundy, P. G. Lagoudakis, A. V. Kavokin, J. J. Baumberg, G. Christmann, R. Butté, E. Feltin, J.-F. Carlin, and N. Grandjean. Room-temperature polariton lasing in semiconductor microcavities. *Phys. Rev. Lett.*, 98:126405, 2007.
- 3 Patrick Serafin, Tim Byrnes, and German V. Kolmakov. Driven dipolariton transistors in y-shaped channels. *Physics Letters A*, 384(34):126855, 2020.
- 4 T. Gao, P. S. Eldridge, T. C. H. Liew, S. I. Tsintzos, G. Stavrinidis, G. Deligeorgis, Z. Hatzopoulos, and P. G. Savvidis. Polariton condensate transistor switch. *Phys. Rev. B*, 85:235102, 2012.
- 5 Rahul Jayaprakash, Kyriacos Georgiou, Harriet Coulthard, Alexis Askitopoulos, Sai K. Rajendran, David M. Coles, Andrew J. Musser, Jenny Clark, Ifor D. W. Samuel, Graham A. Turnbull, Pavlos G. Lagoudakis, and David G. Lidzey. A hybrid organic–inorganic polariton LED. *Light: Science & Applications*, 8(1):1–11, 2019.
- 6 H. Min, R. Bistritzer, J.-J. Su, and A. H. MacDonald. Room-temperature superfluidity in graphene bilayers. *Phys. Rev. B*, 78:121401(R), 2008.
- 7 O. L. Berman, Yu. E. Lozovik, and D. W. Snoke. Theory of Bose-Einstein condensation and superfluidity of two-dimensional polaritons in an in-plane harmonic potential. *Phys. Rev. B*, 77:155317, 2008.
- 8 Oleg L. Berman, Roman Ya. Kezerashvili, and German V. Kolmakov. Harnessing the polariton drag effect to design an electrically controlled optical switch. *ACS Nano*, 8(10):10437–10447, 2014. PMID: 25265156.
- 9 Tim Byrnes, Tomoyuki Horikiri, Natsuko Ishida, and Yoshihisa Yamamoto. Bcs wave-function approach to the bcc-bcc crossover of exciton-polariton condensates. *Physical Review Letters*, 105(18):186402, 2010.
- 10 J. Kasprzak, M. Richard, S. Kundermann, A. Baas, P. Jeambrun, Jonathan Mark James Keeling, F. M. Marchetti, M. H. Szymanska, R. Andre, J. L. Staehli, V. Savona, P. B. Littlewood, B. Deveaud, and Le Si Dang.

Bose-einstein condensation of exciton polaritons. *Nature*, 443(7110):409–414, 2006.

¹¹ Daniele Sanvitto and Stéphane Kéna-Cohen. The road towards polaritonic devices. *Nature Materials*, 15(10):1061–1073, 2016.

¹² Xiaoze Liu, Tal Galfsky, Zheng Sun, Fengnian Xia, Erchen Lin, Yi-Hsien Lee, Stéphane Kéna-Cohen, and Vinod Menon. Strong light-matter coupling in two-dimensional atomic crystals. *Nature Photonics*, 9, 2014.

¹³ Frank Ceballos, Matthew Z. Bellus, Hsin-Ying Chiu, and Hui Zhao. Probing charge transfer excitons in a MoSe₂-WS₂ van der waals heterostructure. *Nanoscale*, 7:17523–17528, 2015.

¹⁴ German V. Kolmakov, Leonid M. Pomirchi, and Roman Ya. Kezerashvili. Toward room-temperature superfluidity of exciton polaritons in an optical microcavity with an embedded MoS₂ monolayer. *J. Opt. Soc. Am. B*, 33(7):C72–C79, 2016.

¹⁵ Hui Deng, Gregor Weihs, Charles Santori, Jacqueline Bloch, and Yoshihisa Yamamoto. Condensation of semiconductor microcavity exciton polaritons. *Science*, 298(5591):199–202, 2002.

¹⁶ Iacopo Carusotto and Cristiano Ciuti. Quantum fluids of light. *Reviews of Modern Physics*, 85(1):299–366, 2013.

¹⁷ P. Szymczak and A. J. C. Ladd. Boundary conditions for stochastic solutions of the convection-diffusion equation. *Phys. Rev. E*, 68:036704, 2003.